MACHINES AND PROCESSES FOR CONTINUOUS MANUFACTURING OF ALIGNED CARBON NANOTUBES FOR TOUGH AND MULTIFUNCTIONAL INTERFACE LAYERS

E. S. Polsen, S. M. Perkins, E. R. Meshot, D. Copic, M. Bedewy, A. J. Hart*
Department of Mechanical Engineering, University of Michigan
2350 Hayward Street, Ann Arbor, MI 48109-2125
*ajohnh@umich.edu

S. Figueredo, R. Guzman de Villoria, S.A. Steiner III, B. L. Wardle
Department of Aeronautics and Astronautics, MIT
77 Massachusetts Avenue, Cambridge, MA 02139

SUMMARY

Owing to the exceptional and anisotropic properties of carbon nanotubes (CNTs), vertically aligned CNT "forests" are a highly attractive thin film material for multifunctional enhancement of composite interfaces. We present two designs for continuous manufacturing of aligned CNT forests, wherein high-quality CNT forests are grown on continuously-fed and recirculating substrates. Subsequent transfer printing of CNT forests to aerospace prepregs achieves significant enhancement in interlaminar toughness and demonstrates scalability and integrability for a wide variety of material systems.

Keywords: carbon nanotube, aligned, manufacturing, continuous, interface, interlaminar, mechanical, toughness, electrical, thermal

INTRODUCTION

Compared to hundred-ton quantities of carbon nanotube (CNT) powders produced commercially each year [1], "forests" of vertically-aligned CNTs offer significant advantages in purity, monodispersity (i.e., uniform diameter and length), and structural order. Therefore, CNT forests are attractive both as bulk CNT materials and as integrated layers in a variety of applications, such as for interlaminar toughening of advanced fiber composites, for improving thermal and electrical transport at interfaces, and for high-density electrochemical energy conversion and storage [2-7]. However, CNT forest growth is traditionally performed in batch-style processes over limited areas, and seamless continuous films are needed to realize these applications at commercial scales and reasonable cost.

Synthesis of CNTs by chemical vapor deposition (CVD) involves decomposition of carbon containing precursors and the consequent self-assembly of graphitic carbon at nanoparticle growth sites [8]. The process of CNT film growth by CVD involves several stages: (1) the catalyst is prepared on a substrate, such as a silicon wafer, metal foil, or advanced fiber; (2) the catalyst is heated and treated chemically, such as by exposure to a reducing atmosphere that causes the catalyst thin film to agglomerate into nanoparticles; (3) the catalyst is exposed to a carbon-containing atmosphere, which

causes formation of the CNTs on the nanoparticles and eventual "liftoff" of CNTs which self-organize into a forest due to crowding; and (4) CNT growth continues by competing pathways between accumulation of "good" (graphitic) and "bad" (amorphous) carbon [9]. To engineer the functional properties of CNT materials such as forests, reaction processes must not only treat these stages independently, but must be accompanied by characterization techniques that enable mapping of the forest characteristics for large sample sizes and populations.

Despite extensive research, the mechanism of CNT growth termination remains unclear. It has been proposed that termination is caused by catalyst poisoning due to formation of an amorphous carbon layer, by diffusion limitation of reactant access to the catalyst, or by decreasing mechanical contact between the CNTs which is required to maintain the self-supporting forest structure [10]. However, single catalyst layers can easily grow aligned CNT forests to several millimeters, while layers of only 100μm or less are useful for multifunctional interfaces, including interlaminar reinforcement of laminated composites. Therefore, even without advances in long-life catalysts, dozens of growth cycles could be achieved from a single catalyst deposition. Since rapid (>> 1 μm/s) CNT forest growth is achieved, functional CNT interlayers can be grown in a few seconds or less.

Low-cost deposition and/or re-use of the catalyst are attractive attributes for continuous production of CNTs since the catalyst represents a signficant component of the cost of CNT growth at large volumes. Illustrated in Fig. 1, there are three major strategies for large-scale CNT forest production: (A) batch re-growth which involves sequential growth and harvesting operations on individual substrates; (B) continuous feeding of a catalyst-coated substrate such as a metal foil or fiber [11]; and (C) continuous growth and delamination using a revolving substrate [12], which enables printing to other substrates such as prepregs and plastics. In the latter case, in order to provide a continuous process within a closed system, the catalyst is reused for several cycles. It has been shown that the growth of aligned CNTs, on crystal structured materials, is generated at the base of the CNTs [13], allowing the catalyst to remain on the substrate after CNT removal for re-use.

SYSTEM DESIGN, MODELING, AND CONSTRUCTION

The continuous growth techniques and systems were designed with several critical performance characteristics in mind, and were built upon our extensive study of batch-style CNT forest growth on centimeter-scale substrates. Based on our prior studies, the use of a decoupled CVD method enables the precise tuning of CNT diameter, structural quality, and growth kinetics of vertically aligned CNT forests [14]. Using this approach, the gas is thermally treated before reaching the catalyst, which creates a polydisperse hydrocarbon atmosphere that is necessary for efficient growth of high-quality CNTs [15]. The catalyst-coated substrate is heated locally in a "cold wall" manner. Additionally, since the complete growth cycle undergoes distinct stages that are temporally separated in a batch process, each stage must be spatially maintained within a single apparatus to allow for continuous growth. Thus, each phase would need to occur in a separate spatial zone in order to sequentially achieve pre-treatment of the CNT growth catalyst, CNT growth, and optional printing to another substrate such as a graphite/epoxy prepreg. If the catalyst is to be re-used, careful removal of the CNT forest from the moving substrate must leave the catalyst behind, where it is

subsequently re-used for a large number of cycles, avoiding costly re-application of catalyst each time. Fig. 2 illustrates the overall flow diagram for the continuous growth process that incorporates catalyst activation and re-activation, CNT growth, and CNT removal.

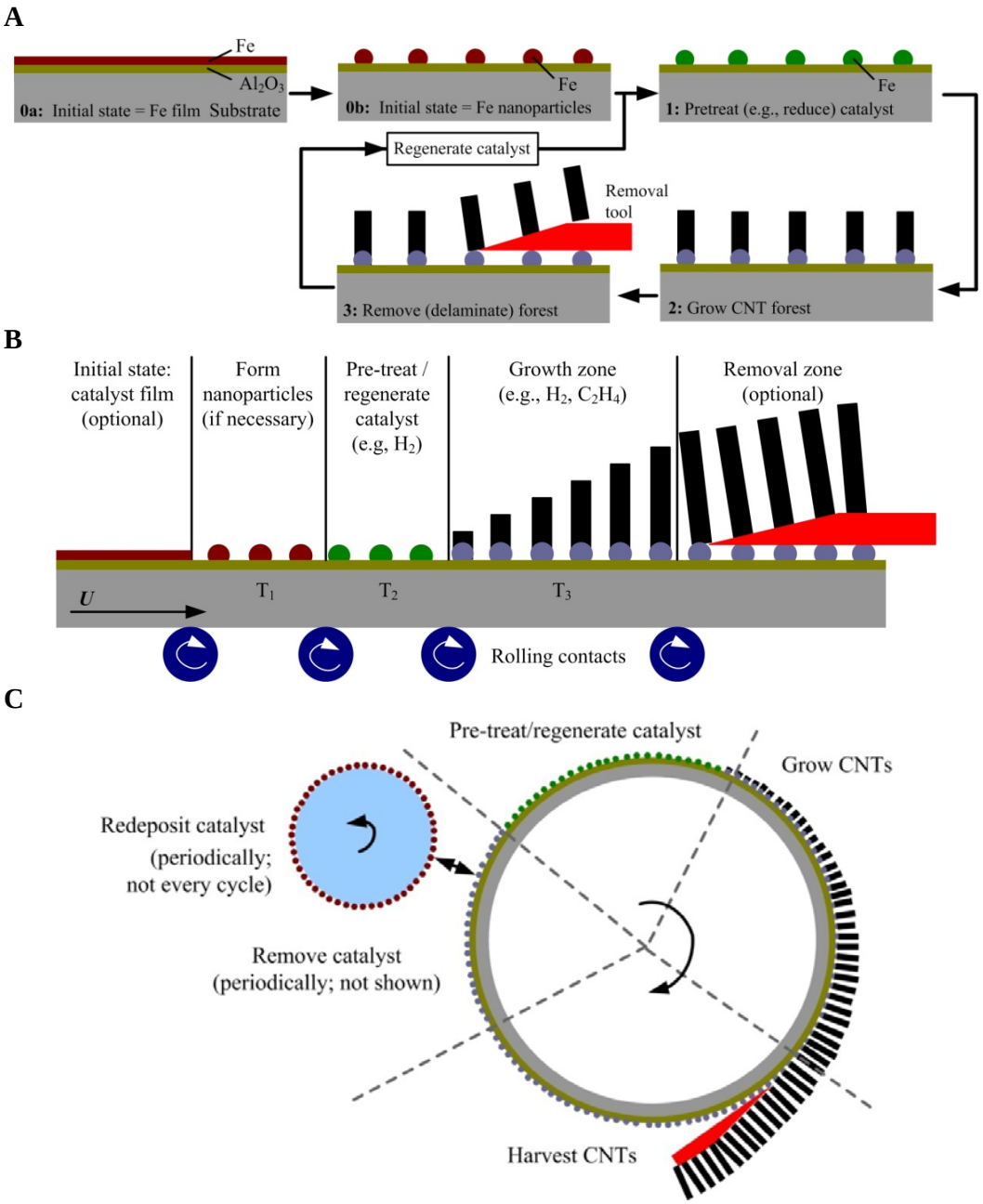

Fig. 1. Continuous aligned CNT forest manufacturing approaches. A) Batch re-growth on individual substrates, B) Continuous feed of a catalyst-coated foil or fiber weave through a heated zone, and C) Catalyst re-use on a re-circulating substrate, with optional catalyst re-application.

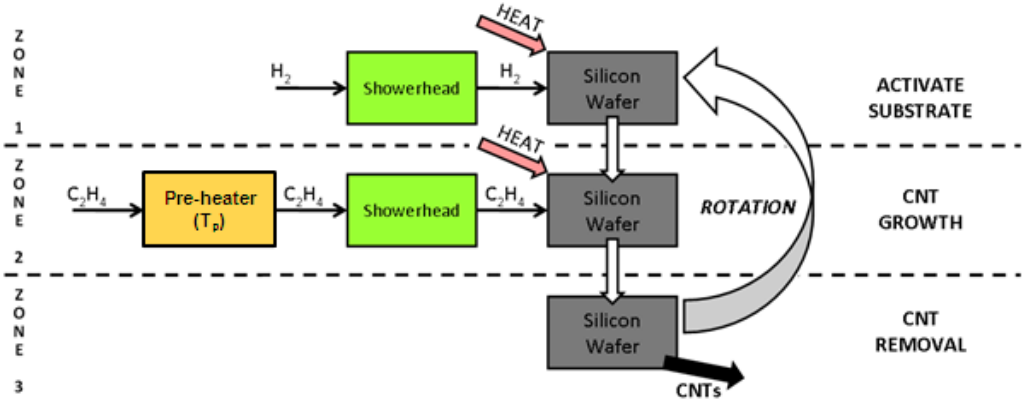

Fig. 2. Process flow diagram for continuous CNT forest growth.

Utilizing the key characteristics mentioned above, we have created a desktop machine for studying continuous production of seamless CNT forests, wherein a circular substrate is rotated through a three-zone, atmospheric-pressure CVD reactor. Shown in Fig. 3, the circular growth substrate is located below a quartz plate that allows for the chamber to be sealed, and for the substrate to be heated via radiation. The use of a ceramic disc coupled with heating elements achieves uniformity and control of the substrate temperature (T_s). Catalyst annealing, CNT growth and delamination from the substrate occur individually in their respective zones as the substrate rotates continuously. Also, additional ports along the walls of the growth chamber allow installation of thermocouples, or for connection of a mass spectrometer for online chemical analysis of the reaction atmosphere.

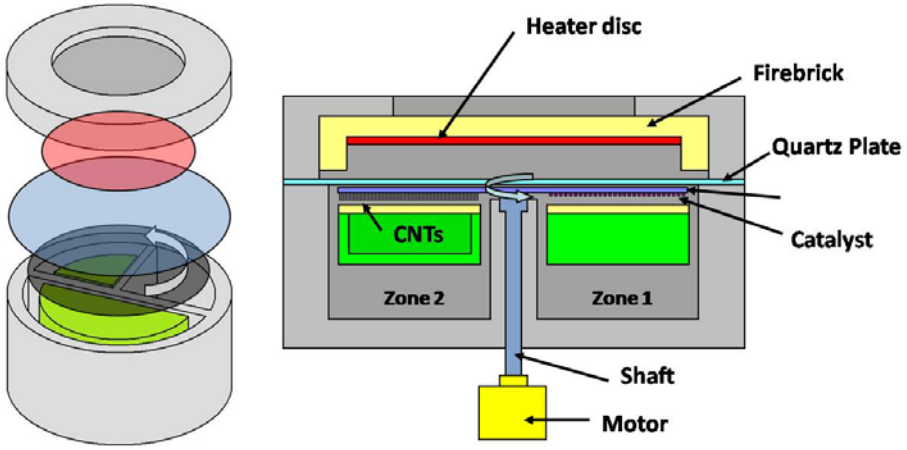

Fig. 3. Schematic design of the continuous CNT forest growth machine.

The processing chamber is constructed from 6013 aluminum, with an outer diameter of 10.5”, 1.25” thick side walls, and an overall height of 3.6” with a bottom floor thickness of 1” (Fig. 4). In order to separate the chamber into three zones, there are internal separating walls that rise to a height of 2” above the bottom floor of the chambers. Each of the separating walls features a hollow center, with ports at the

bottom of the chamber for exhausting the reactant gases. This design allows for minimal mixing of the gases from each zone so as to retain three separate environments. All ports for reactant gas entry into the device are located at the bottom of the chamber along with the exit ports, thus allowing the sides of the chamber to be smooth and easily insulated. Each of the inlet ports leads to a single porous alumina-capped, stainless steel showerhead, for each zone, that allows even distribution of the gases over the growth substrate.

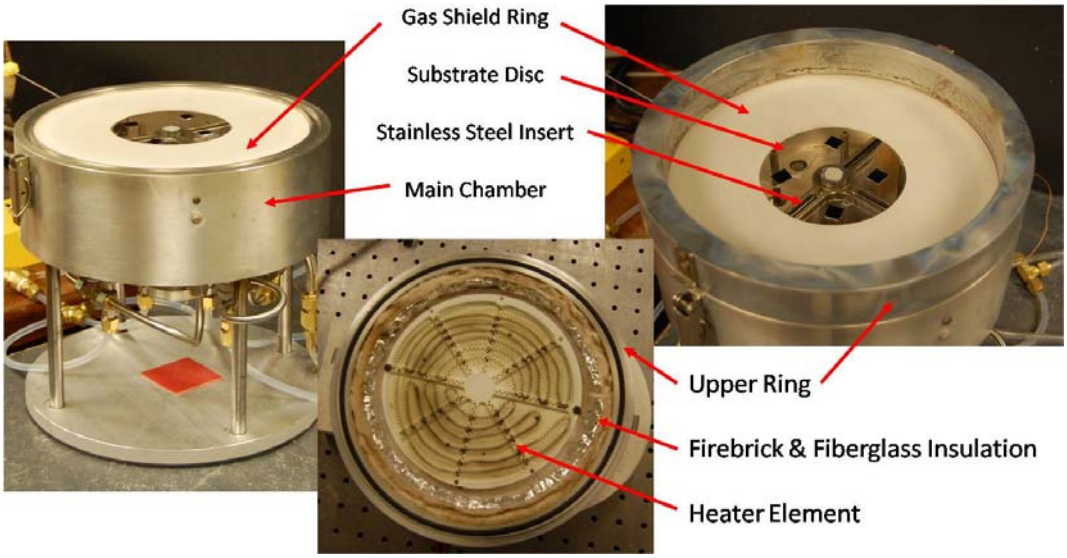

Fig. 4. Desktop continuous CNT forest growth machine. Substrate wafer is replaced with a 4" quartz disc and centimeter size catalyst samples for testing.

Although the device was designed to handle up to a 6" diameter wafer for growth, a 4" diameter substrate wafer is more suitable based on current catalyst deposition methods. A 0.5" diameter 303 stainless steel slug is bonded to the center of the silicon wafer and then pinned to a central shaft that runs through the bottom of the chamber. Sealed by a polyurethane lip seal, and supported by PTFE sleeve bearings, the shaft is connected to a NEMA 17 Hybrid step motor at the bottom of the chamber to provide continuous rotation at low speeds. In order to minimize flow of reactant gases into the space above the substrate wafer, a quartz ring is located at the same height as the wafer with 0.03" clearance around the circumference of the wafer. The entire chamber is then sealed with Viton o-rings and a 10.25" diameter quartz disc.

While the quartz disc seals off the bottom chamber from the surrounding environment, it also allows for the wafer to be heated from above via radiation. A 6013 aluminum cap for the lower chamber allows for a clamping mechanism to apply pressure to the Viton o-rings around the quartz plate, as well as an interior space that houses a set of heating elements. The heating elements are nickel-chromium wire, laced through an alumina disc that provides a high emissivity for radiating the heat to the wafer. In order to maintain a relatively high temperature gradient across the chamber cap, firebrick is located between the heater and the aluminum cap. The heater is controlled via a PID controller and a phase angle SCR, with a thermocouple feedback loop.

Flows, heat fluxes, and temperatures within the CNT manufacturing process were analyzed through thermal (Fig. 5) and CFD models developed using RadTherm and FLUENT software packages. These models capture the boundary conditions within the chambers of the apparatus during CNT growth, and allow tradeoff studies to be conducted with regards to different structural and insulation materials. The thermal model predicted that with a heater disc temperature of 1075°C, the wafer temperature would reach 850°C, while the outer aluminum surface of the main chamber would reach 291°C. Validation of the thermal model, based on initial tests conducted with the chamber using K-Type thermocouples for temperature measurements, revealed that the model accurately predicted the surface temperature of the chamber, but over-predicted the wafer temperature for a given heater output. The wafer temperature during operation only reached 650°C, most likely due to radiation heat loss from the wafer to the walls of the chamber. Thus, the thermal model needs to be refined further in regards to radiation surface properties to generate a validated model from current data so that future design modifications can be modeled accurately. In order to mitigate this loss, a firebrick case around the outside of the chamber will be designed, along with a new material for the lower chamber to withstand the elevated temperature.

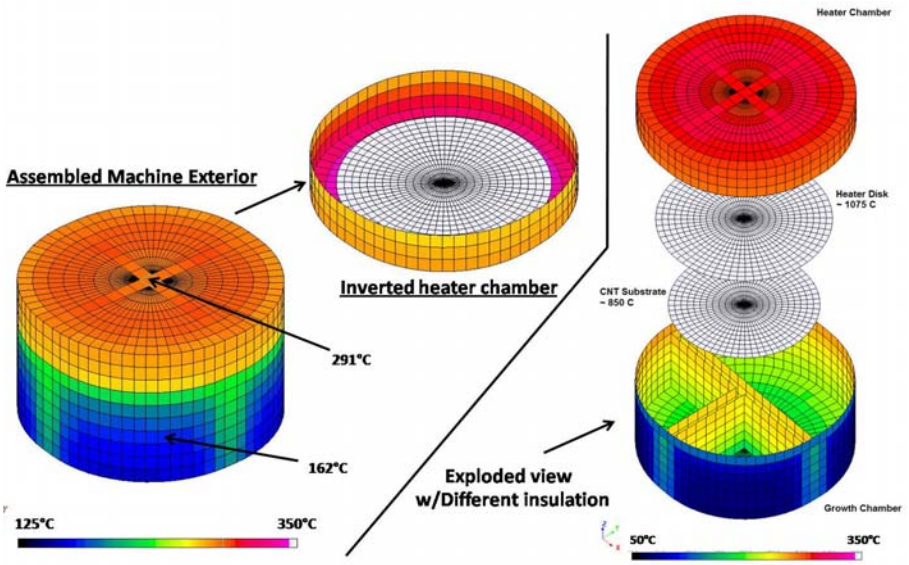

Fig. 5. RadTherm thermal modeling results, predicting chamber and wafer surface temperatures.

CNT GROWTH METHODS

The method for growing aligned forests by continuous methods is analogous to the batch style process that we have studied extensively [14,16], except the processing steps are separated spatially by rotation of the substrate. A silicon wafer, coated with a supported catalyst film of 1/10 nm Fe/Al_2O_3 deposited by electron beam evaporation, is loaded into the chamber. The chamber is then purged with He to establish an inert atmosphere before the wafer is heated. After the silicon wafer is heated, the annealing zone receives a mixture of He and H_2, and the growth zone receives a mixture of He, H_2 and C_2H_4. During the first rotation of the substrate, only areas of the wafer that

have been annealed for a long enough period of time will experience growth. Thus, the first CNTs to be removed will be present in the de-lamination zone after roughly ½ of a rotation. Once in this zone, the CNTs are removed through mechanical means via a sharp edge to separate the forests from the substrate, and the process repeats.

CNT GROWTH RESULTS

The temperature of catalyst annealing, which is equal to T_s, by exposure to a reducing atmosphere before growth, is a principal means of controlling the CNT diameter. Upon heating in H_2 and He, the Fe film agglomerates almost instantaneously into well-defined nanoparticles, as verified by AFM imaging (Figure 6a,b). Thin film theory also predicts that the mean particle size will increase as T_s increases, so that the free energy of the particles decreases [17-19]. Many previous studies have shown correlations between particle size and resultant CNT diameter [20,21]. After initial heating, the particles coarsen slowly and increase in size with continued exposure to H_2, yielding fewer and larger particles at longer catalyst annealing times. Upon introduction of C_2H_4, CNTs are templated by the catalyst nanoparticles; when a relatively high density of particles are active [22], CNTs crowd and form a vertically-aligned configuration which accommodates continued upward growth as carbon is added at the catalyst which resides on the substrate.

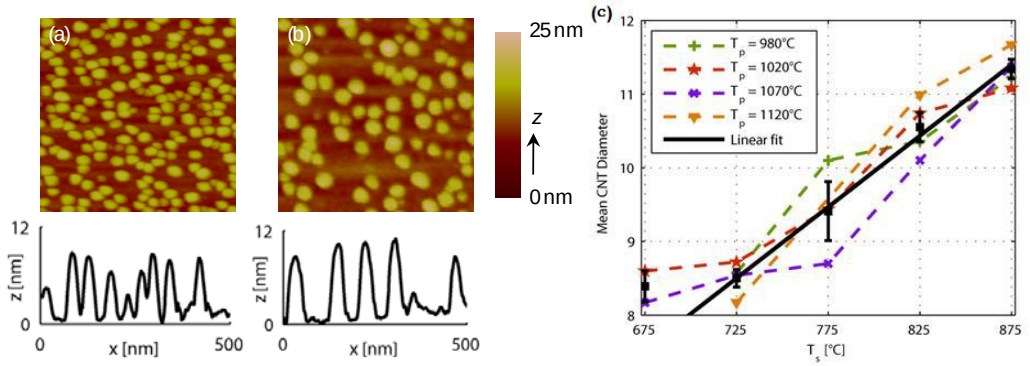

Fig. 6. CNT growth results, obtained by batch processing using decoupled thermal treatment of the hydrocarbon precursor and catalyst substrate. AFM images (500 nm × 500 nm) and corresponding topographical profiles of Fe/Al_2O_3 catalyst film, after annealing in H_2/He for 2 minutes at (a) T_s = 725°C and (b) T_s = 875°C. (c) Correlation between T_s and diameter is observed over a wide range of T_p values.

The activity of the reactant mixture, determined by T_p, has a negligible effect on CNT diameter (Figure 6c). Mapping the CNT forests by small-angle X-ray scattering (SAXS) and the use of TEM imaging, reveals that the average CNT diameter is directly related to T_s. A linear relationship is apparent from T_s = 725°C-875°C, and CNT diameters values appear to be constant for T_s = 725°C and below. Further, the distribution of diameters broadens with increasing T_s. CNT diameter dependence on T_s, which overlaps for a wide range of T_p, demonstrates that the diameter is not strongly influenced by the gas phase rearrangement of C_2H_4 but rather is driven by the thermal treatment of the catalyst. Thus, wide-range tuning of CNT diameter from 5-30

nm can be achieved by controlling the duration and atmosphere of catalyst annealing, and this can be implemented in a fully continuous fashion.

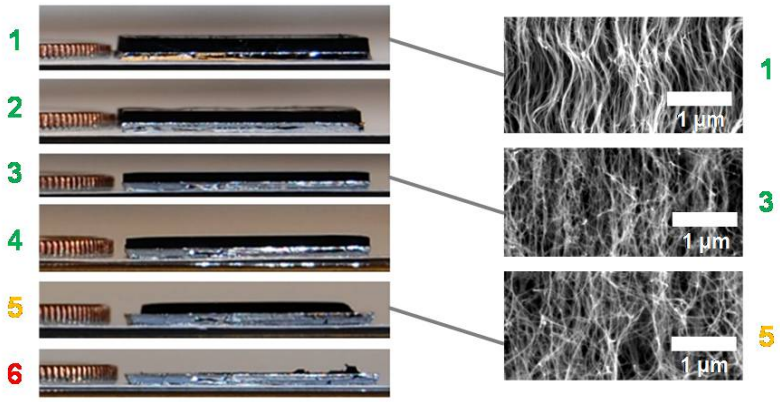

Fig. 7. Visual and SEM imagery of the MWNT forests after each growth cycle, verifying catalyst reactivation yet showing degradation of CNT forest height, density and alignment.

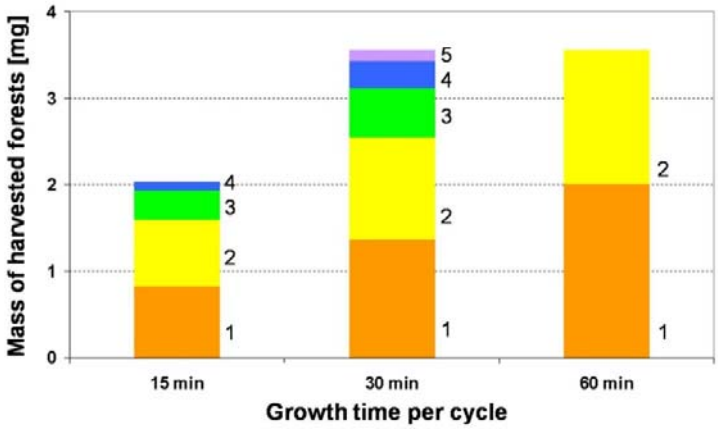

Fig. 8. Mass of CNT forests harvested with repeated cycles at three selected growth durations.

Batch growth of CNT forests on centimeter sized substrates using the standard batch CVD recipe was used to investigate the performance of the thin film catalyst after consecutive growth and delamination operations. After each growth cycle, the CNTs were delaminated, using a razor blade to mechanically propagate a crack at the substrate surface, and then placed in the tube furnace and the same CVD process was repeated. This study was executed for several different growth durations, and each case was iterated until a CNT forest did not grow during the most recent cycle. The CNT areal density and alignment decreased with each consecutive growth cycle, along with the forest height (Fig. 7). Additionally, the total CNT yield, defined as the mass of

harvested forests for the total number of cycles, depended on the duration of the individual growth cycles (Fig. 8).

Finally, as an initial step toward CNT growth on continuously fed fibers and tows, we demonstrate CNT forest growth on a silicon substrate that is resistively heated by rolling through a resistively heated zone using a second machine design (Fig. 9) [23]. Further investigation of the limiting mechanisms of catalyst performance, so as to optimize the continuous feeding and catalyst recycling process to maintain uniform CNT forest characteristics at rapid rates and over large cycle life, is ongoing.

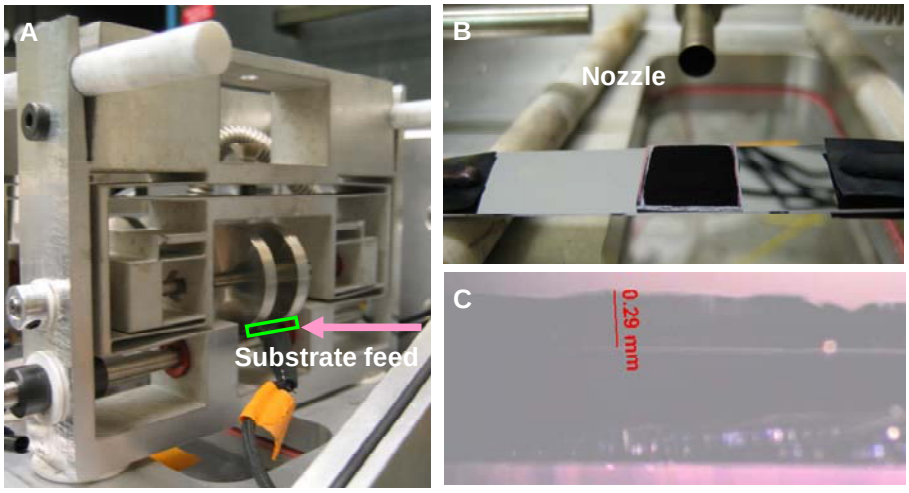

Fig. 9. Moving feed CNT forest growth: (A) apparatus with rolling substrate leading to the heating zone; (B) directed gas delivery; (C) optical images of forest sidewall.

CONCLUSIONS

Utilizing a decoupled thermal process with the continuous growth will enable the precise tuning of CNT diameter, structural quality, and growth kinetics of vertically aligned CNT forests. Additionally, batch catalyst re-use experiments showed that a single deposition of catalyst could be reused for five cycles in the proper growth environments, allowing the continuous process to potentially process five complete wafers of aligned CNT forests without catalyst re-deposition. Utilization of roll-to-roll printing to prepregs from the continuous process will allow the CNT forests to be directly applied to laminated composites. As our previous studies have shown, interlaminar reinforcement of traditional graphite-epoxy composites with as-grown forests of 10nm diameter MWNTs increases Mode I and II toughness of composite laminates by up to 100-300% [2]. Mechanical densification, capillarity-driven polymer infiltration, and roll-to-roll transfer enable integration of large-area CNT forests on application-relevant substrates, while preserving the essential growth conditions necessary for high-quality CNTs [24].

ACKNOWLEDGEMENTS

This work is supported by the National Science Foundation (CMMI-0800213), Airbus S.A.S., Boeing, Embraer, Lockheed Martin, Saab AB, Spirit AeroSystems, Textron

Inc., Composite Systems Technology, and TohoTenax through MIT's Nano-Engineered Composite aerospace STructures (NECST) Consortium, and the University of Michigan Department of Mechanical Engineering and College of Engineering. We thank Stephanie Chien, Seline Soh, and Chunyi Yeo for working on design and fabrication of the recirculating growth chamber during the Winter 2008 ME450 Design and Manufacturing III Course at the University of Michigan.

References

1. P.C. Eklund, et al., International Assessment of Research and Development on Carbon Nanotubes: Manufacturing and Applications. WTEC, 2006, http://wtec.org/cnm.
2. Baughman, R. H.; Zakhidov, A. A.; de Heer, W. A., *Science* **2002,** *297* (5582), 787-792.
3. Garcia, E. J.; Wardle, B. L.; Hart, A. J., *Composites Part A* **2008,** *39* (6), 1065-1070.
4. Endo, M.; Hayashi, T.; Kim, Y.; Terrones, M.; Dresselhaus, M., *Philosophical Teansactions of the Royal Society A* **2004,** *362* (1823), 2223-2238.
5. Tong, T.; Zhao, Y.; Delzeit, L.; Kashani, A.; Meyyappan, M.; Majumdar, A., *IEEE Transactions on Components and Packaging Technologies* **2007,** *30* (1), 92-100.
6. Blanco, J., Garcia, E.J., Guzman deVilloria, R., and B.L. Wardle, *J. Composite Materials* **2009**, 43 (8).
7. Wardle, B.L., *17th International Conference on Composite Materials (ICCM)* **2009**, Edinburgh, Scotland.
8. Kong, J.; Soh, H.; Cassell, A.; Quate, C.; Dai, H., *Nature* **1998,** *395* (6705), 878-881.
9. Lacava, A. I.; Bernardo, C. A.; Trimm, D. L., *Carbon* **1982,** *20* (3), 219-223.
10. Bedewy, M.; Meshot, E.; Guo, H.; Verploegen, E.; Lu, W.; Hart, A.J., Submitted for publication **2009**.
11. Yamamoto, N.; Hart, A.J.; García, E.J.; Wicks, S.S.; Duong, H.M.; Slocum, A.H.; Wardle, B.L., *Carbon* **2009**, 47 (3), 551-560.
12. Hart, A.J.; Slocum, A. H.; Wardle, B. L.; Garcia, E. J., Continuous process for the production of nanostructures including nanotubes, PCT/US2006/041239.
13. Ago, H.; Ishigami, N.; Yoshihara, N.; Imamoto, K.; Akita, S.; Ikeda, K.; Tsuji, M.; Ikuta, T.; Takahashi, K., *Journal of Physical Chemistry C* **2008,** 112, 1735-1738.
14. Meshot, E.; Plata, D.; Tawfick, S.; Zhang, Y.; Verploegen, E.; Hart, A.J., Submitted for publication **2009**.
15. Hart, A. J.; van Laake, L.; Slocum, A. H., *Small* **2007,** *3* (5), 772-777.
16. Hart, A.J.; Slocum, A.H., *Journal of Physical Chemistry B* **2006**, 110 (16), 8250-8257.
17. Ardell, A. J. In *Experimental confirmation of the Lifshitz-Wagner theory of particle coarsening*, The Mechanism of Phase Transformations in Crystalline Solids, University of Manchester, University of Manchester, 1968.
18. Atwater, H. A.; Yang, C. M., *Journal of Applied Physics* **1990,** *67* (10), 6202-6213.
19. Thompson, C. V., *Acta Metallurgica* **1988,** *36* (11), 2929-2934.
20. Kukovitsky, E. F.; L'Vov, S. G.; Sainov, N. A.; Shustov, V. A.; Chernozatonskii, L. A., *Chemical Physics Letters* **2002,** *355* (5-6), 497-503.
21. Nerushev, O. A.; Dittmar, S.; Morjan, R. E.; Rohmund, F.; Campbell, E. E. B., *Journal of Applied Physics* **2003,** *93* (7), 4185-4190.
22. Figueredo, S.L.; Guzman deVilloria, R.; Hart, A.J.; Steiner III, S.A.; Slocum, A.H.; Wardle, B.L., 9th *International Conf. of the European Society for Precision Engineering and Nanotechnology (EUSPEN)* **2009**, San Sebastian, Spain.
23. Bennett, R. D.; Hart, A. J.; Cohen, R. E., *Advanced Materials* **2006,** *18* (17), 2274.
24. Wardle, B.L.; Saito, D.S.; García, E.J.; Hart, A.J.; de Villoria, R.G.; Verploegen, E.A., *Advanced Materials* **2008,** 20 (14), 2710-2714.